

David Taylor Model Basin Naval Surface Warfare Center, Carderock Division

9500 MacArthur Boulevard
West Bethesda, Maryland 20817-5700

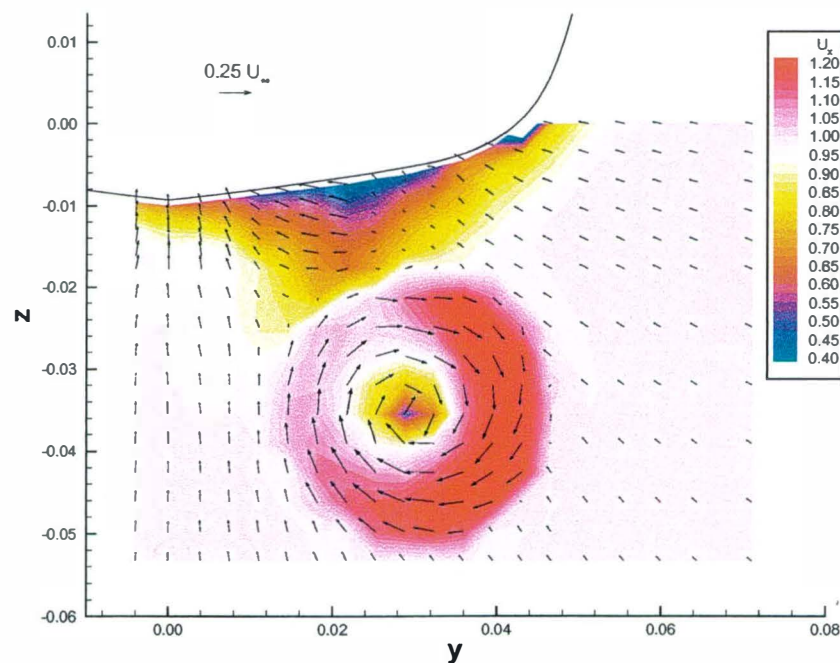
NSWCCD-50-TR-2005/012

JUNE 2005

HYDROMECHANICS DEPARTMENT REPORT

Propeller Flow Field Mapping of Model 5415 using 3-Component Laser Doppler Velocimetry

By
Christopher Chesnakas
Toby Ratcliffe



Approved for Public Release; Distribution Unlimited.



**DEPARTMENT OF THE NAVY
NAVAL SURFACE WARFARE CENTER
CARDEROCK DIVISION**

**CARDEROCK DIVISION HEADQUARTERS
DAVID TAYLOR MODEL BASIN
9500 MACARTHUR BOULEVARD
WEST BETHESDA, MD 20817-5700**

IN REPLY REFER TO:

5605
5200/2005048
JUN 29 2005


From: Commander, Carderock Division, Naval Surface Warfare Center
To: Office of Naval Research (Pat Purtell, Code 333)

Subj: FORWARDING OF REPORT

Encl: (1) NSWCCD-50-TR-2005/012 "Propeller Flow Field Mapping
Of Model 5415 using 3-Component Laser Doppler
Velocimetry" by Christopher Chesnakas and Toby
Ratcliffe, June 2005
(2) Customer Project Survey Form 5000-20A (Rev 5)

1. Enclosure (1) is forwarded for your information and retention.
2. It is requested that enclosure (2) be completed and returned to Carderock Division, Naval Surface Warfare Center. Customer surveys are conducted at the completion of a project and are used at the Department level to control and verify the system process capability. The forms will be reviewed for customer comments, including complaints and recommendations. Corrective actions will be taken.

WILLIAM G. DAY, JR.
By direction

Copy to:
University of Michigan (R. Beck)
University of Iowa (F. Stern)
(J. Longo)
SAIC/San Diego (D. Wyatt)
NSWC Panama City (M. Hyman)
ARL (E. Patterson)
DTIC 

DOCUMENT RECEIPTDate: 28 June 2005**TO:**

DTIC
8725 John J. Kingman Rd Ste 0944
Ft. Belvoir VA 22060-6218

FROM:

**Naval Surface Warfare Center, Carderock Division,
9500 MacArthur Blvd
Code 5200
West Bethesda, MD 20817-5700**

The following material is transmitted for official use:

NSWCCD-50-TR-2005/012 "Propeller Flow Field Mapping of Model 5415 using a
3-Component Laser Doppler Velocimetry" by Christopher Chesnakas and Toby
Ratcliffe, June 2005

UNCLASSIFIED

1 Copy

Please sign and return

Date of Receipt _____ Signature and Title _____

REPORT DOCUMENTATION PAGE

Form Approved
OMB No. 0704-0188

Public reporting burden for this collection of information is estimated to average 1 hour per response, including the time for reviewing instructions, searching existing data sources, gathering and maintaining the data needed, and completing and reviewing this collection of information. Send comments regarding this burden estimate or any other aspect of this collection of information, including suggestions for reducing this burden to Department of Defense, Washington Headquarters Services, Directorate for Information Operations and Reports (0704-0188), 1215 Jefferson Davis Highway, Suite 1204, Arlington, VA 22202-4302. Respondents should be aware that notwithstanding any other provision of law, no person shall be subject to any penalty for failing to comply with a collection of information if it does not display a currently valid OMB control number. PLEASE DO NOT RETURN YOUR FORM TO THE ABOVE ADDRESS.

1. REPORT DATE (DD-MM-YYYY) June 2005		2. REPORT TYPE Research and Development-Dec 1999		3. DATES COVERED (From - To)	
4. TITLE AND SUBTITLE Propeller Flow Field Mapping of Model 5415 using 3-Component Laser Doppler Velocimetry				5a. CONTRACT NUMBER	
				5b. GRANT NUMBER	
				5c. PROGRAM ELEMENT NUMBER	
6. AUTHOR(S) Christopher Chesnakas and Toby Ratcliffe				5d. PROJECT NUMBER	
				5e. TASK NUMBER	
				5f. WORK UNIT NUMBER 99-1-5200-053	
7. PERFORMING ORGANIZATION NAME(S) AND ADDRESS(ES) Naval Surface Warfare Center Carderock Division, Code 5200 9500 MacArthur Boulevard West Bethesda, Maryland 20817				8. PERFORMING ORGANIZATION REPORT NUMBER NSWCCD-50-TR-2005/012	
9. SPONSORING / MONITORING AGENCY NAME(S) AND ADDRESS(ES) ONR Code 333 800 North Quincy Street Arlington, Virginia 22217				10. SPONSOR/MONITOR'S ACRONYM(S)	
				11. SPONSOR/MONITOR'S REPORT NUMBER(S)	
12. DISTRIBUTION / AVAILABILITY STATEMENT Distribution Unlimited - Approved for Public Release					
13. SUPPLEMENTARY NOTES					
14. ABSTRACT <i>Subsurface velocities were obtained on Model 5415 using a three-component Laser Doppler Velocimetry System. Data was obtained for the model running at a Froude number of 0.28, which corresponds to a full scale ship speed of 20 knots. Measurements were performed in three planes, $x/L=0.9367$ (propelled), $x/L=0.9453$ (unpropelled), and $x/L=0.9603$ (propelled and unpropelled). A detailed uncertainty analysis was performed. The dominant source of uncertainty is the precision uncertainty due to the long period fluctuations in the flow. Over most of the flow field, the turbulence is low, and the uncertainty in any velocity component is less than 0.8% of U_{∞}. In high turbulence regions of the flow, such as the hull or propulsor wakes, the uncertainty can increase to 2.5% of U_{∞}. Both axial velocities and rms velocities are presented for each of the measurement planes. The effect of the propeller on the flow at the farthest downstream measurement plane is quantified.</i>					
15. SUBJECT TERMS Laser Doppler Velocimetry, Propelled Wake, Nominal Wake					
16. SECURITY CLASSIFICATION OF: Unclassified			17. LIMITATION OF ABSTRACT	18. NUMBER OF PAGES 26	19a. NAME OF RESPONSIBLE PERSON Toby Ratcliffe
a. REPORT Unclassified	b. ABSTRACT Unclassified	c. THIS PAGE same as report			19b. TELEPHONE NUMBER (include area code) 301-227-7018

TABLE OF CONTENTS

	Page
ABSTRACT	1
ADMINISTRATIVE INFORMATION	1
INTRODUCTION	1
MODEL INFORMATION	1
EXPERIMENTAL APPARATUS	4
LDV system	4
<u>Probes and Strut</u>	4
<u>Signal Processing</u>	7
<u>Seeding</u>	7
<u>Traverse</u>	7
EXPERIMENTAL PROCEDURE	7
TEST CONDITIONS	8
DATA REDUCTION	9
<u>Coordinate Transformations</u>	9
<u>Strut Interference Corrections</u>	9
UNCERTAINTY ANALYSIS	10
Elemental Uncertainties	10
Calculated Uncertainties	10
RESULTS	15
CONCLUSIONS	21

LIST OF FIGURES

	Page
1 - Model 5415 with Removable Appendages (shafts and struts)	2
2 - DTMB Propellers 4876 and 4877 on Model	2
3 - Fiber-optic probes and strut	5
4 - Probes and strut in dry dock	5
5 - Position of LDV strut and hull	6
6 - Regions of flow where measurements are blocked	6
7 - LDV measurement stations	8
8 - Contours of axial velocity uncertainty, $x/L = 0.9367$, propelled	13
9 - Contours of axial velocity uncertainty, $x/L = 0.9453$, nominal wake	13
10 - Contours of axial velocity uncertainty, $x/L = 0.9603$, nominal wake	14
11 - Contours of axial velocity uncertainty, $x/L = 0.9603$, propelled	14
12 - Contours of axial velocity, $x/L = 0.9367$, propelled	17
13 - Contours of rms velocity, $x/L = 0.9367$, propelled	17
14 - Contours of axial velocity, $x/L = 0.9453$, nominal wake	18
15 - Contours of rms velocity, $x/L = 0.9453$, nominal wake	18
16 - Contours of axial velocity, $x/L = 0.9603$, nominal wake	19
17 - Contours of rms velocity, $x/L = 0.9603$, nominal wake	19
18 - Contours of axial velocity, $x/L = 0.9603$, propelled	20
19 - Contours of rms velocity, $x/L = 0.9603$, propelled	20
20 - Propelled minus nominal wake, $x/L = 0.9603$	21

LIST OF TABLES

	Page
1 - Model 5415 Dimensions and Particulars	3
2 – Propeller Operating Conditions	3
3 - LDV Measurement Planes and Conditions	9
4 - Elemental uncertainties	10

SYMBOLS

B	Bias uncertainty
D	Propeller diameter = 22.10 cm
L	Length of hull at waterline
n	Propeller Rotational Speed
P	Precision (random) uncertainty
q	Root-mean-square (RMS) fluctuation of velocity, $TKE = \rho q^2/2$, normalized by U_∞
$U(U_i)$	Total uncertainty in velocity component U_i , normalized by U_∞
U_x	Velocity in direction of model axis, normalized by U_∞ (+ downstream)
U_y	Velocity in horizontal direction, perpendicular to model axis, normalized by U_∞ (+ starboard)
U_z	Velocity in vertical direction, normalized by U_∞ (+ up)
U_∞	Model speed
x	Coordinate along hull axis, from bow waterline, normalized by L
y	Coordinate in transverse direction, from centerline, normalized by L (+ starboard)
z	Coordinate vertical direction, from waterline, normalized by L (+ up)
θ_2	Angle between measured velocity component 2 and z axis
θ_3	Angle between measured velocity component 3 and z axis

BLANK

ABSTRACT

Subsurface velocities were obtained on Model 5415 using a three-component Laser Doppler Velocimetry System. Data were obtained for the model running at a Froude number of 0.28, which corresponds to a full scale ship speed of 20 knots. Measurements were performed in three planes, $x/L=0.9367$ (propelled), $x/L=0.9453$ (unpropelled), and $x/L=0.9603$ (propelled and unpropelled). A detailed uncertainty analysis was performed. The dominant source of uncertainty is the precision uncertainty due to the long period fluctuations in the flow. Over most of the flow field, the turbulence is low, and the uncertainty in any velocity component is less than 0.8% of U_∞ . In high turbulence regions of the flow, such as the hull or propulsor wakes, the uncertainty can increase to 2.5% of U_∞ . Both axial velocities and rms velocities are presented for each of the measurement planes. The effect of the propeller on the flow at the farthest downstream measurement plane is quantified.

ADMINISTRATIVE INFORMATION

The work described in this report was performed by the Propulsor Systems Division of the Hydrodynamics Department, Carderock Division, Naval Surface Warfare Center. The work was sponsored by the Office of Naval Research, Mechanics and Energy Conversion S&T Division (Code 333) under the Hydrodynamics Task of FY99 Surface Ship Technology Program (PE602121N). The work was performed under work unit 99-1-5200-053.

INTRODUCTION

An ONR Free Surface Flow Initiative for validating and transitioning Reynold's Averaged Navier Stokes computational codes was begun in 1995. Model 5415 was chosen as a representative naval combatant hull form on which a detailed set of experimental data would be obtained. This report documents the subsurface velocities obtained on Model 5415. This work was accomplished during March and April of 1999.

MODEL INFORMATION

Model 5415 was built of wood in 1980 to a linear scale ratio of 24.824 and is representative of a modern naval combatant hull form. Electronic files representing the geometry of the hull form, both bare hull and with appendages can be downloaded from the Model 5415 web site (<http://www.dt.navy.mil/hyd/sur-shi-mod/index.html>). Figure 1 shows a photograph of the stern of the model, fully outfitted for this experiment with removable appendages (shafts and struts). The model has twin rudders which are set at an angle of zero degrees relative to the model centerline. The model was not fitted with bilge keels. Turbulence stimulator studs 3.2 mm in diameter and 2.5 mm in height were fitted to the model in accordance with Hughes and Allen¹.

¹ Hughes, C. and J. F. Allen, "Turbulence Stimulation on Ship Models" Society of Naval Architects and Marine Engineers (SNAME) Transactions, Vol. 59 (1951).

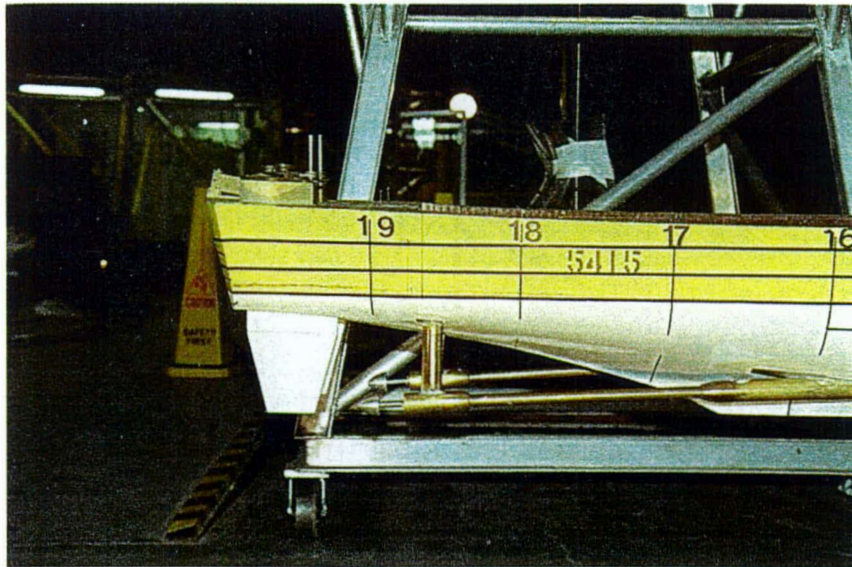


Figure 1 – Model 5415 with Removable Appendages (shafts and struts)

During the propelled experiments, the model was fitted with design propellers designated as DTMB propellers 4876 and 4877. These represent 5.49-meter full-scale diameter propellers. A photograph of the propellers on the model is shown in Figure 2. Figure 3 shows an isometric view of the appended model. Table 1 provides model dimensions and other particulars, including the model sinkage and trim for these experiments and Table 2 documents the propeller operating conditions during the collection of this data.



Figure 2 – DTMB Propellers 4876 and 4877 on Model

Table 1 – Model 5415 Dimensions and Particulars

Lambda	24.824
LBP , LWL	5.72 m
Displacement	548.8 kg
Appended Wetted Surface	4.92 m ²
Sinkage at FP (Fn=0.28)	-0.0027L
Sinkage at AP (Fn=0.28)	-0.00086L
Sinkage at FP (Fn=0.41)	-0.00054L
Sinkage at AP (Fn=0.41)	-0.0083L
Propellers	Port 4877 Starboard 4876
Propeller Diameter	22.10 cm

Table 2 – Propeller Operating Conditions

*(K_T and K_Q determined from open water tests;
D is propeller diameter, n is revolutions per minute)*

Speed, V (m/sec)	K_T= T/(ρD⁴n²)	K_Q= Q/(ρD⁵n²)	RPM	J=V/nD
2.06	0.178	0.0461	436	1.28

EXPERIMENTAL APPARATUS

LDV system

Probes and Strut

The LDV system consisted of two TSI Model 9832 fiber-optic probes attached to each other on a streamlined strut as shown in Figs. 3 and 4. The probes were mounted rigidly together on the strut in order to keep the measurement volumes aligned. In order to measure at different points in the flow, the probes could be translated in a plane perpendicular to the model axis as a unit.

The upper probe in Fig. 3 used the green (514.5 nm) and blue (488 nm) beams of an argon-ion laser to measure two components of velocity, U_1 and U_2 , and the lower probe used the violet (476.5 nm) beams of the laser to measure a third component, U_3 . The probes are oriented with their axes parallel to the flow direction (the x axis), and have prisms at the front lens to deflect the beams by 90° . The probes have 50 mm beam spacing and 350 mm focal length (air) lenses. Each probe has an elliptical probe volume with a major axis of 0.9 mm and both minor axes of 0.06 mm. The probe volumes are approximately 420 mm from the probe centerlines in water, which, as seen in Fig. 5, keeps the strut and probes away from the hull.

The fringe spacing for the green, blue, and violet beams was $3.7022\mu\text{m}$, $3.5325\mu\text{m}$, and $3.4765\mu\text{m}$, respectively. The probes were oriented so that the green channel measured the axial component of velocity, U_1 , the blue channel measured a velocity component U_2 perpendicular to the x axis and at 15.77° to the z axis, and the violet channel measured a velocity component U_3 perpendicular to the x axis and at 65.43° to the z axis. These angles were designed to give maximum access to the flowfield while keeping the strut and probes as far from the model as possible. Even so, there were some regions in the flow which were blocked from view of the beams by the shaft. As seen in Fig. 6, the shaft will block measurements of U_1 and U_2 on the inboard side of the shaft, and the shaft will block measurements of U_3 above and to the inboard side of the shaft. In both these regions, the secondary (in plane) velocities cannot be calculated. Axial (perpendicular to plane) velocity cannot be calculated only in the inboard region.

The strut consisted of 3×6 inch aluminum extrusions bolted together in an L shape. On the leading edge of the strut, a circular fairing is attached. At the trailing edge, a 6.5-inch streamlined fairing is attached.

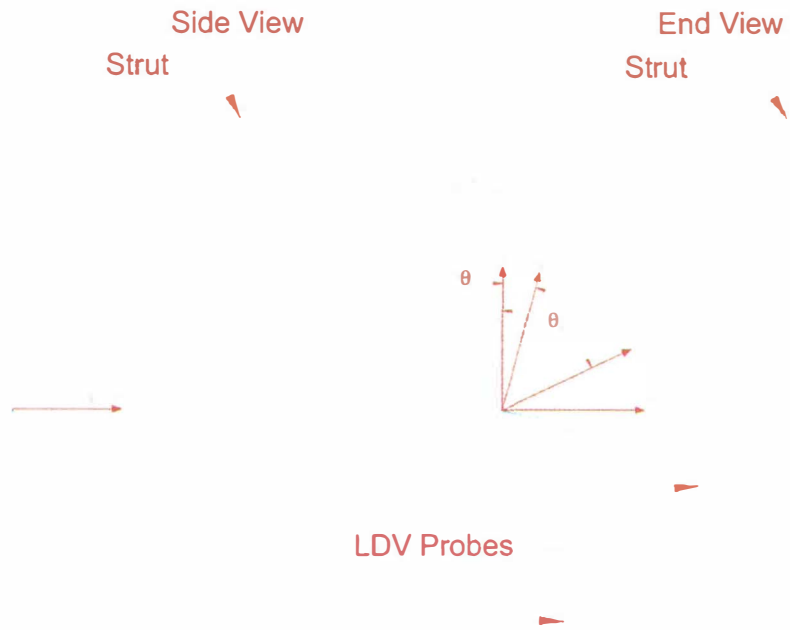


Figure 3 - Fiber-optic probes and strut

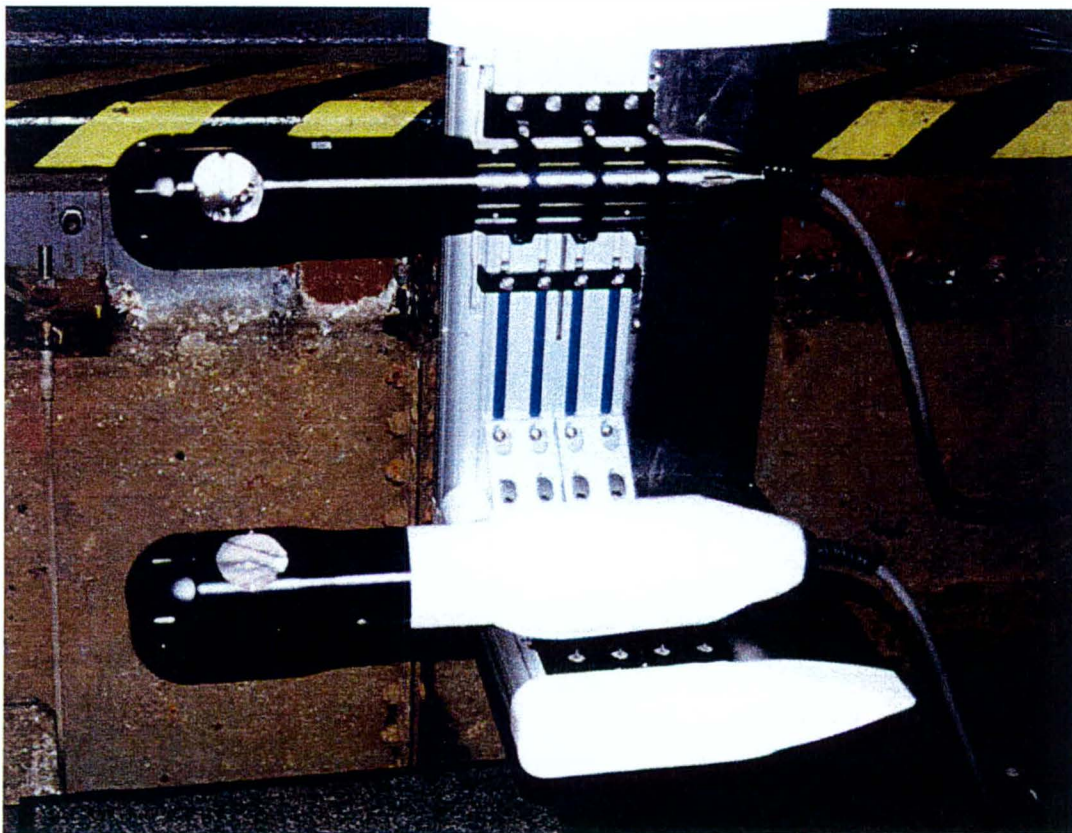


Figure 4 - Probes and strut in dry dock

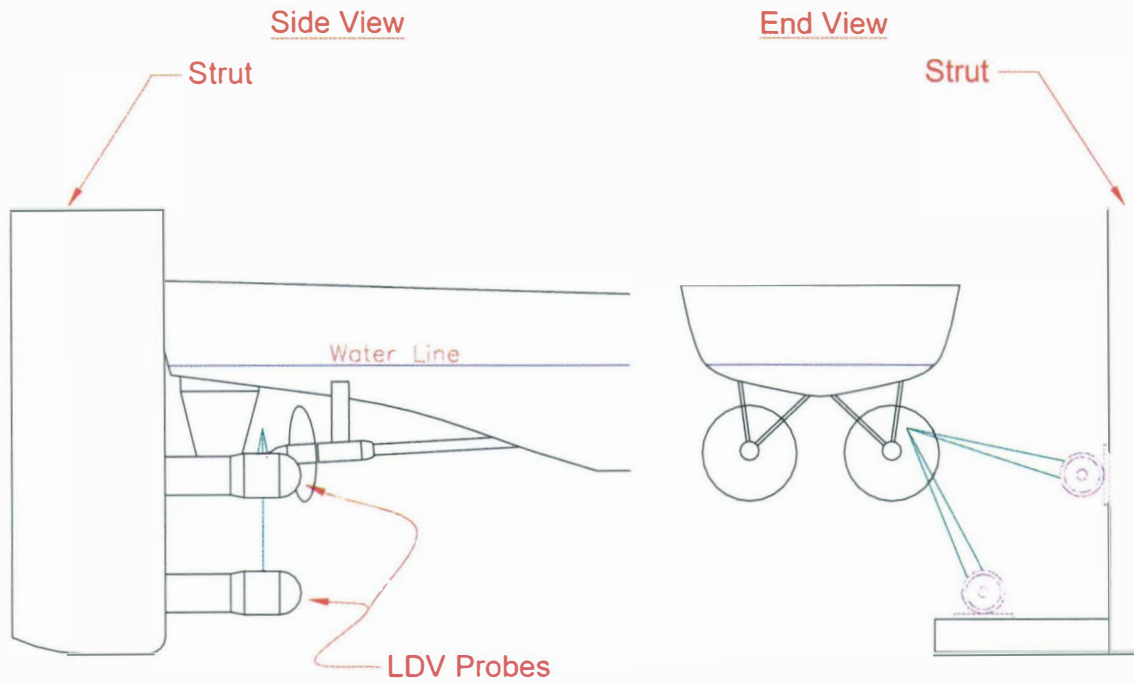


Fig 5 - Position of LDV strut and hull

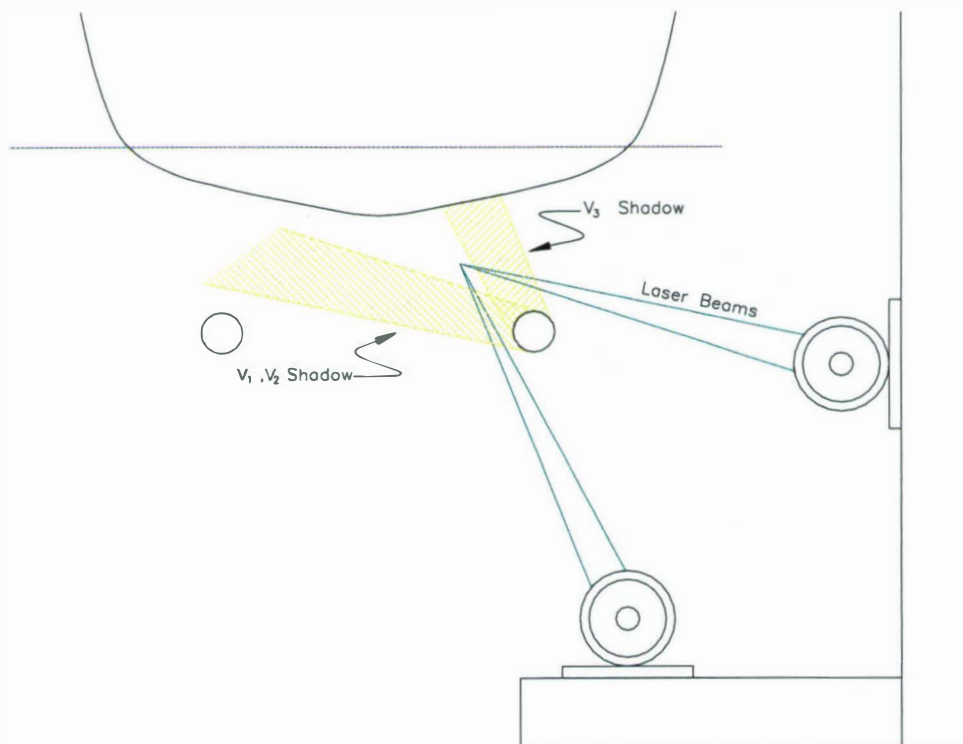


Fig 6 - Regions of flow where measurements are blocked

Signal Processing

Doppler signals were analyzed with a TSI Model IFA 655 Digital Burst Correlator. The processor performs a 256-sample, double-clipped, autocorrelation on each doppler burst, allowing the measurement of velocity even when the signal-to-noise ratio is low. In order to maximize data rate, the processors were operated in the random mode.

Seeding

The flow about the hull was seeded with 6000-grit silicon carbide powder. The powder was mixed into a slurry with water and injected through seven 0.1-inch diameter taps in the hull at $x/L = 0.2$.

Traverse

The strut assembly was attached to the carriage through a two-component, computer controlled traverse. The traverse sat on the carriage, above the water level. The traverse was powered by two stepper motors attached to 5-thread-per-inch lead screws. Position was determined by counting the pulses used to drive the stepper motors.

The traverse could move the probes in the y and z directions. Positioning in the x direction was achieved by manually moving the hull on the center rail of the carriage. The range of movement in the y direction was approximately 19 inches, and in the z direction the measurement volume could be positioned to approximately 20 inches below the water surface.

EXPERIMENTAL PROCEDURE

Before data was acquired, it was first necessary to obtain the position of the LDV measurement volume. This was done by using a reference mark on the side of the hull, just below the waterline. At each axial location the hull was positioned fore and aft to bring the reference mark into the plane of the laser beams, and then adjusted for the proper dynamic sinkage and trim for the test speed. Once the hull was locked onto the rail, the traverse was then moved in the y and z directions to bring the beam crossing onto the mark.

At each axial location, between 245 and 407 points in the flow were measured. Since the travel of the traverse in the y direction was limited to only 19 inches, only the starboard side of the flowfield

was measured. During each carriage pass, the strut assembly was moved to different positions under computer control. Between 10 and 40 points could be obtained in each pass, depending on the data rate. In general, positions near the hull had higher data rates than positions away from the hull, since the seed was injected into the hull boundary layer.

At each measurement point in the flow, 10000 velocity realizations were acquired. Data rate was generally nearly equal for all velocity components, so that the number of data points on each channel was approximately 3300.

TEST CONDITIONS

Measurements on Model 5415 were all performed at 20 knots full scale, 4.01 knots model scale. Three axial locations were measured as shown in Fig. 7. They are: just ahead of the propeller at $x/L = 0.9367$, in the plane of the propeller at $x/L = 0.9453$, and just aft of the propeller at $x/L = 0.9603$. All the measurements were with the propulsor operating at the self propulsion point. Sinkage and trim were fixed at the proper dynamic levels for design draft. The measurement conditions are summarized in Table 3.

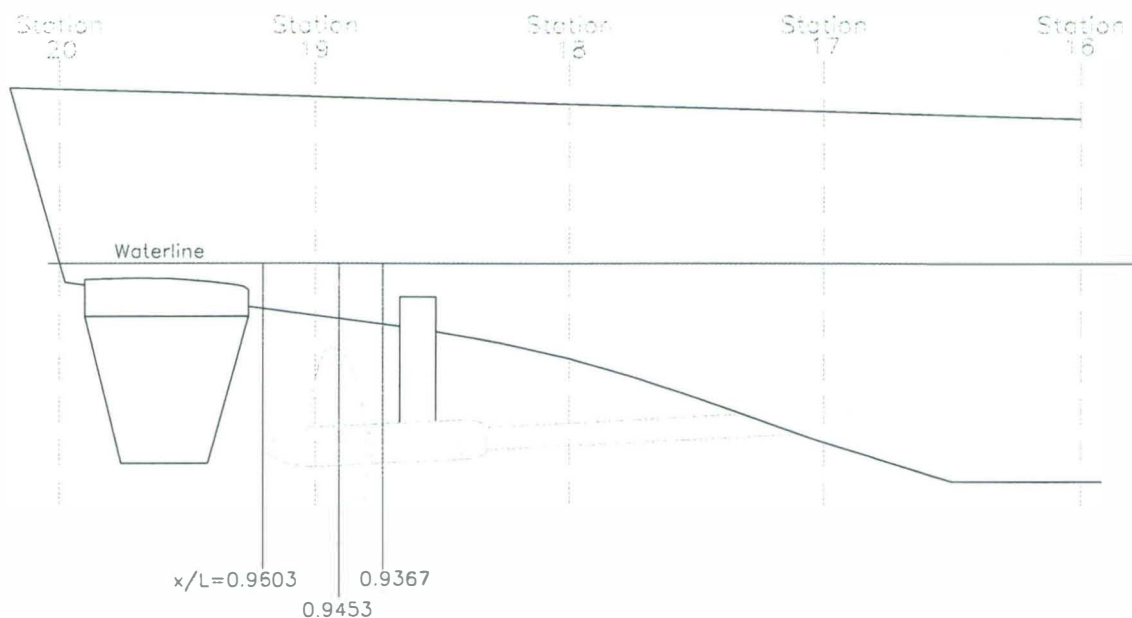


Figure 7 - LDV measurement stations

Table 3 - LDV Measurement Planes and Conditions

Condition	x/L	Speed (kt.)		Prop. RPM	Num. Pts.
		Model	Full		
Propelled	0.9367	4.01	20.0	436	407
Nominal Wake	0.9453	4.01	20.0		245
Propelled	0.9603	4.01	20.0	436	295
Nominal Wake	0.9603	4.01	20.0		295

DATA REDUCTION

Coordinate Transformations

Three components of velocity, U_1 , U_2 , and U_3 , were measured with the present system, but the components were not aligned with the x , y , and z axes of the model, nor were they perpendicular. The relation between the measured components and the model axes defined by the angles of the two probe axes to the horizontal, θ_2 and θ_3 . These angles are 15.77° and 65.43° , respectively. The measured velocities are transformed to the model coordinates by

$$U_x = U_1 \quad (1)$$

$$U_y = \frac{-U_2 \cos \theta_3 + U_3 \cos \theta_2}{\sin(\theta_3 - \theta_2)} \quad (2)$$

$$U_z = \frac{U_2 \sin \theta_3 - U_3 \sin \theta_2}{\sin(\theta_3 - \theta_2)} \quad (3)$$

Strut Interference Corrections

Although the measurement volume was some distance from the probes and strut, there was still some disturbance of the measured flow by the hardware. The disturbance was quantified by measuring the water velocity with no model attached. If there is no disturbance of the flow, U_1 should measure the carriage speed, and U_2 and U_3 should be zero. A correction to bring the no-model velocities to their ideal values was calculated and then applied to the measurements of the flow around the model. The corrections are:

$$U_{x \text{ corrected}} = \frac{U_{x \text{ raw}}}{0.9753 - 0.2815 z/L} \quad (4)$$

$$U_{y \text{ corrected}} = U_{y \text{ raw}} + U_{x \text{ corrected}} (0.042 - 0.124 z / L) \quad (5)$$

$$U_{z \text{ corrected}} = U_{z \text{ raw}} + U_{x \text{ corrected}} \left(0.003 - (z / L + 0.0488)^2 \cdot 4.06 \right) \quad (6)$$

UNCERTAINTY ANALYSIS

Elemental Uncertainties

The uncertainties for the fundamental quantities measured in this experiment are listed in Table 4. Those uncertainties which are the same for all measurements are listed as bias uncertainties, and those uncertainties which vary for each measurement are listed as precision uncertainties. Uncertainties are listed as a fraction of the nominal value, unless otherwise noted.

The uncertainties in x , y , and z are the uncertainties in positioning the probe volume with respect to the model. The Δx , Δy , and Δz uncertainties are the uncertainties in positioning the three probe volumes with respect to each other, with the position of the second measured component defined for the purpose of calculation to be the measurement point. Uncertainty in the measurement of the frequency is assumed to be small relative to the uncertainty due to finite sample size, and so is ignored.

Table 4 - Elemental uncertainties.

UNCLASSIFIED					
Item	Bias	Precision	Item	Bias	Precision
U_{∞}	0.0001	0.0001	$\Delta x (U_2 - U_1)$	0.000009 L	
n	0.001	0.002	$\Delta y (U_2 - U_1)$	0.000009 L	
d_f	0.003		$\Delta z (U_2 - U_1)$	0.000009 L	
x	0.00022 L		$\Delta x (U_2 - U_3)$	0.000026 L	
y	0.00022 L		$\Delta y (U_2 - U_3)$	0.000026 L	
z	0.00022 L		$\Delta z (U_2 - U_3)$	0.000026 L	
θ_2, θ_3	0.08°				

Calculated Uncertainties

The calculated uncertainties are found from combining the above component uncertainties along with information on the flow conditions. The bias uncertainty arises from bias in the measured components of velocity, uncertainty in the relative component positions, uncertainty in the component angles, and velocity bias. For example, for the z -component of velocity, the bias uncertainty is:

$$\begin{aligned}
B^2(U_z) = & \left(\frac{\partial U_z}{\partial U_2} B(U_2) \right)^2 + \left(\frac{\partial U_z}{\partial U_3} B(U_3) \right)^2 + \left(\frac{\partial U_z}{\partial U_3} \frac{\partial U_3}{\partial y} B(\Delta y_{23}) \right)^2 + \left(\frac{\partial U_z}{\partial U_3} \frac{\partial U_3}{\partial z} B(\Delta z_{23}) \right)^2 \\
& + \left(\frac{\partial U_z}{\partial \theta_2} B(\theta_2) \right)^2 + \left(\frac{\partial U_z}{\partial \theta_3} B(\theta_3) \right)^2 + (Strut Bias)^2
\end{aligned} \tag{7}$$

No term for Δx is included in the equation since velocity gradients in the x direction are assumed to be small.

Strut bias arises due to the uncertainty in the corrections made to the measured velocity described in the *Strut Interference Corrections* section. This bias was estimated to be $0.006U_\infty$ for each component.

Precision, or random uncertainty arises due to fluctuations in the measured velocity. Normally, this would be calculated as the standard deviation of the mean velocity (the RMS velocity divided by the square root of the number of measurements). However, the random uncertainty for these measurements is greater. The flow appeared to have low frequency fluctuations that were similar in period to the period over which the measurements were acquired. Since the period of these fluctuations was unknown, this uncertainty was estimated by examining the scatter of repeat measurements. From these repeated measurements, the precision uncertainty for a velocity component is estimated as $P(U_i) = 0.1 q$. The resultant total uncertainty for each component of velocity, $U(U_i)$, is then:

$$U^2(U_x) = B(U_1)^2 + \left(\frac{\partial U_x}{\partial y} B(\Delta y_{12}) \right)^2 + \left(\frac{\partial U_x}{\partial z} B(\Delta z_{12}) \right)^2 + (0.006U_\infty)^2 + 0.01q^2 \tag{8}$$

$$\begin{aligned}
U^2(U_y) = & \left(\frac{\cos \theta_3}{\sin(\theta_3 - \theta_2)} B(U_2) \right)^2 + \left(\frac{\cos \theta_2}{\sin(\theta_3 - \theta_2)} B(U_3) \right)^2 + \left(\frac{\cos \theta_2}{\sin(\theta_3 - \theta_2)} \frac{\partial U_3}{\partial y} B(\Delta y_{23}) \right)^2 \\
& + \left(\frac{\cos \theta_2}{\sin(\theta_3 - \theta_2)} \frac{\partial U_3}{\partial z} B(\Delta z_{23}) \right)^2 + \left[\left(\frac{-U_3 \sin \theta_2}{\sin(\theta_3 - \theta_2)} + \frac{U_y}{\tan(\theta_3 - \theta_2)} \right) B(\theta_2) \right]^2 \\
& + \left[\left(\frac{U_2 \sin \theta_3}{\sin(\theta_3 - \theta_2)} - \frac{U_y}{\tan(\theta_3 - \theta_2)} \right) B(\theta_3) \right]^2 + (0.006U_\infty)^2 + 0.01q^2
\end{aligned} \tag{9}$$

$$\begin{aligned}
U^2(U_z) = & \left(\frac{\sin \theta_3}{\sin(\theta_3 - \theta_2)} B(U_2) \right)^2 + \left(\frac{\sin \theta_2}{\sin(\theta_3 - \theta_2)} B(U_3) \right)^2 + \left(\frac{\sin \theta_2}{\sin(\theta_3 - \theta_2)} \frac{\partial U_3}{\partial y} B(\Delta y_{23}) \right)^2 \\
& + \left(\frac{\sin \theta_2}{\sin(\theta_3 - \theta_2)} \frac{\partial U_3}{\partial z} B(\Delta z_{23}) \right)^2 + \left[\left(\frac{-U_3 \cos \theta_2}{\sin(\theta_3 - \theta_2)} + \frac{U_z}{\tan(\theta_3 - \theta_2)} \right) B(\theta_2) \right]^2 \\
& + \left[\left(\frac{U_2 \cos \theta_3}{\sin(\theta_3 - \theta_2)} - \frac{U_z}{\tan(\theta_3 - \theta_2)} \right) B(\theta_3) \right]^2 + (0.006 U_\infty)^2 + 0.01 q^2
\end{aligned} \tag{10}$$

Since the uncertainty of the measurements is dependent on the conditions of the flow, it is not possible to assign a single number to the velocity uncertainty. Instead, the uncertainty was calculated at all points in the flow. At almost all points, the dominant source of uncertainty is the precision uncertainty due to the long period fluctuations in the flow. This uncertainty is the same for all three components of velocity, so the total uncertainty for the three components is nearly identical. For this reason, only plots of the total uncertainty are shown, and only for a single component of velocity. Plots of the total axial-velocity uncertainty are shown for all stations in Figs. 8-11. Over most of the flow field, the turbulence is low, and the uncertainty in any velocity component is less than 0.8% of U_∞ . In high turbulence regions of the flow, such as the hull or propulsor wakes, the uncertainty can increase to 2.5% of U_∞ . The scattered regions of very high uncertainty in Figs. 8 and 9 are due to points for which the laser beams for one measured component were partially blocked by the shaft. These anomalous regions should be ignored.

Uncertainty in the root-mean-square of the velocity fluctuations, q , was dominated by the long term velocity fluctuations in the flow. This made for a precision uncertainty of $0.03q$. It should be noted, however, that the LDV has a lower noise floor, below which it can not measure the turbulence. For this setup, the noise floor in q was approximately 1.5% of the measured velocity.

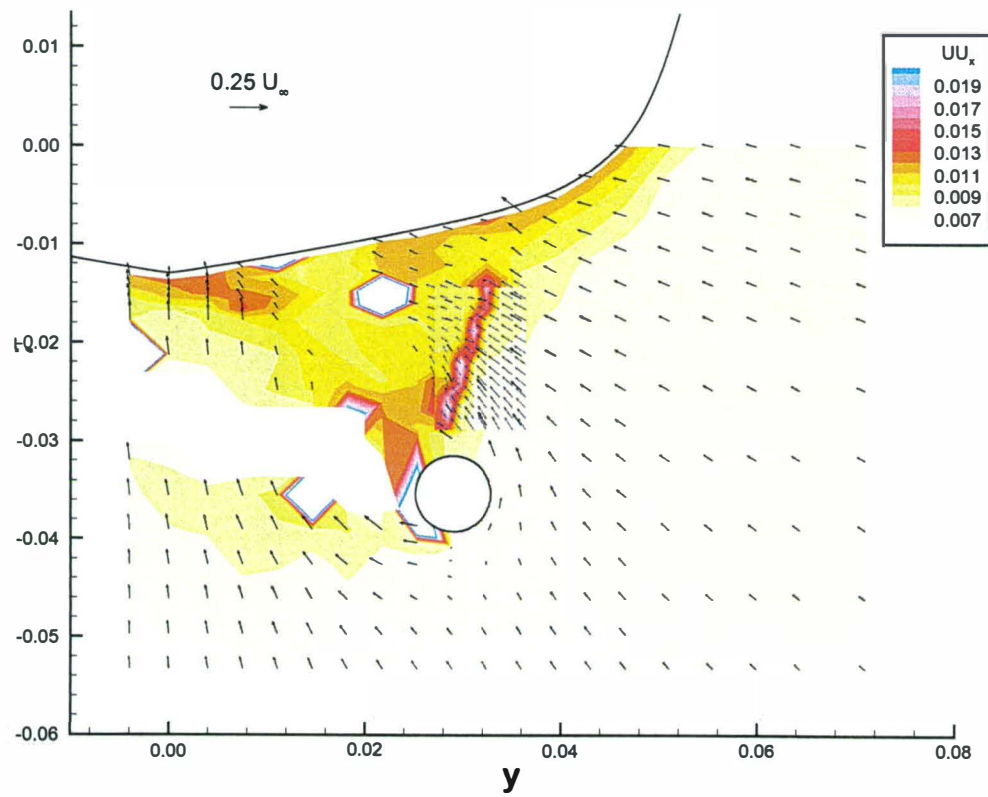


Figure 8 - Contours of axial velocity uncertainty, $x/L = 0.9367$, propelled

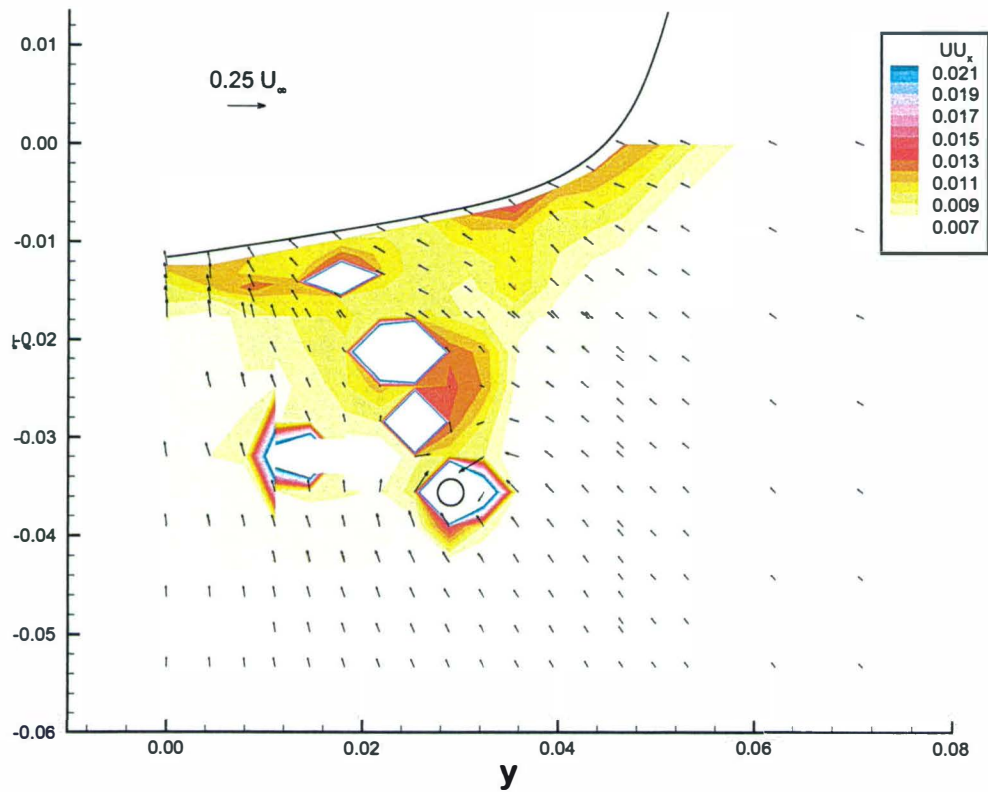


Figure 9 - Contours of axial velocity uncertainty, $x/L = 0.9453$, nominal wake

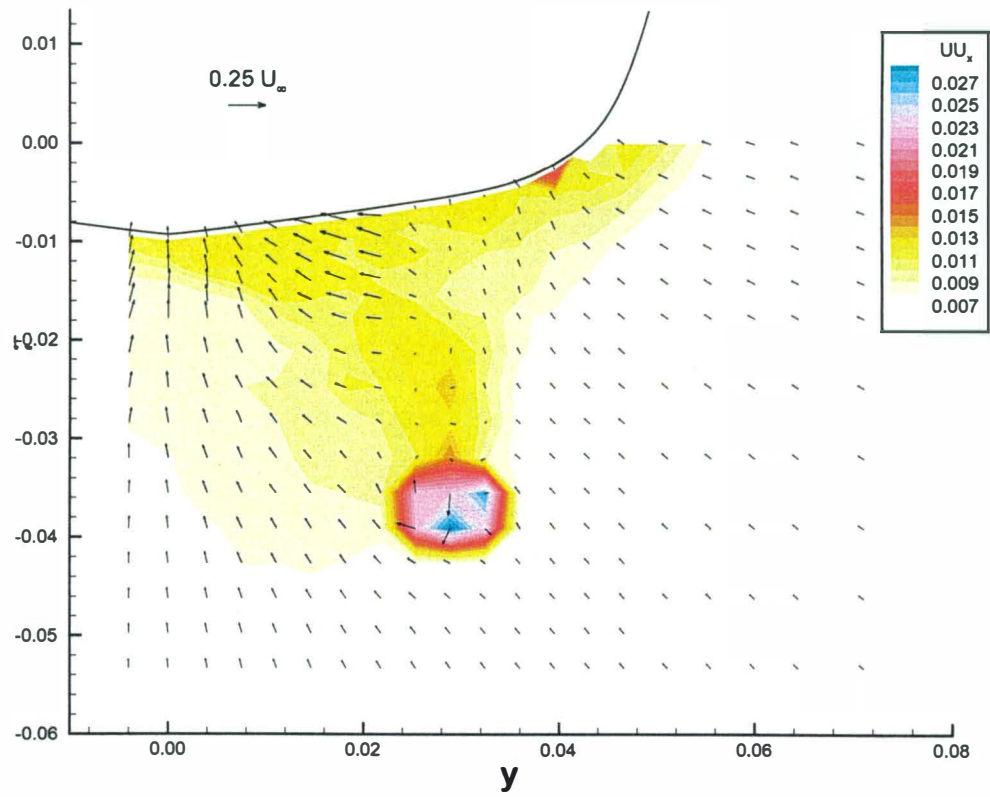


Figure 10 - Contours of axial velocity uncertainty, $x/L = 0.9603$, nominal wake

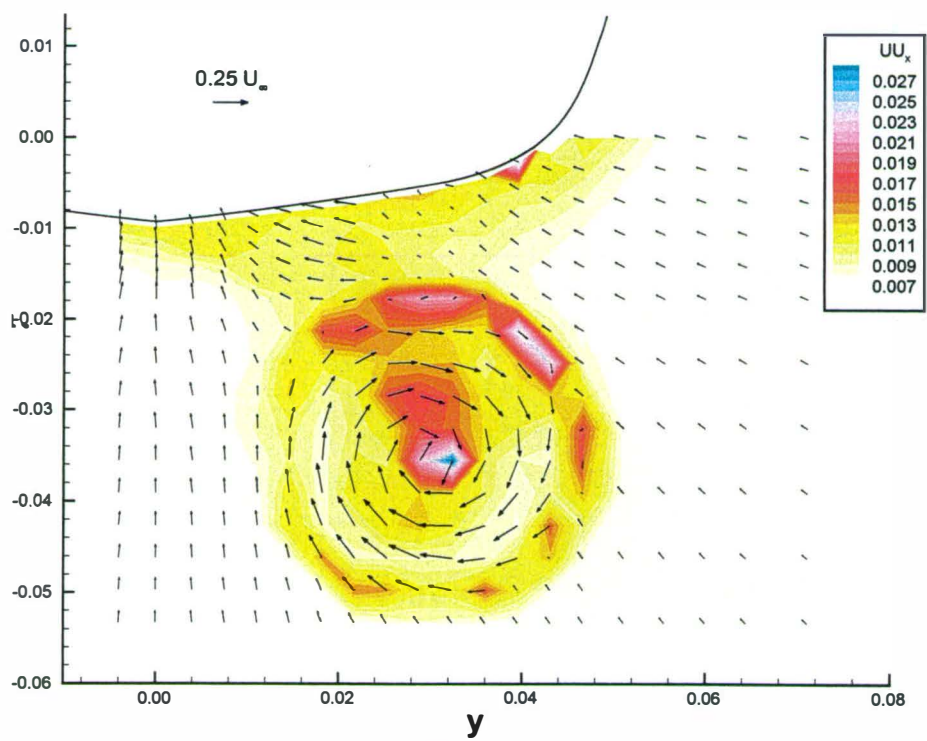


Figure 11 - Contours of axial velocity uncertainty, $x/L = 0.9603$, propelled

RESULTS

Measurements were obtained in a grid of points at each plane as outlined in the *Experimental Procedure* section. At these planes, plots are shown with color contours of the velocity component in the direction of the model axis, U_x . Plots are also shown with color contours of the rms of the velocity fluctuations, q , which reveal the viscous wakes in the flowfield. Note that $\rho q^2/2$ is equal to the turbulent kinetic energy. On top of the color contours are vectors of the in-plane velocities, looking upstream. In all plots, velocities are normalized by the ship speed, U_∞ , and distances are normalized by the ship length, L .

The flow just ahead of the propeller, at $x/L = 0.9367$, is shown in Figs. 12 and 13. The white circle in the middle of the plots is the location of the propeller hub, and the regions above and inboard of the hub are missing measurements of one or more of the velocity components due to blockage of the laser beams. The contours of axial velocity clearly show the hull boundary layer. The V-strut wakes are less well defined, since the thin wakes generally fall in between the grid of measurement points. The region of the outboard strut was measured in a finer grid in order to better resolve the strut wakes, but the contours in this region still are somewhat lumpy. An even finer measurement grid would be needed in this region to adequately resolve the strut wake profile. Very little effect is seen from the shaft.

Similar results are seen in the plot of rms velocity, q , in Fig. 13, with the strut wake being a little more distinct than in the velocity plot and the hull boundary layer being a little more confused, due to the lack of data for two components above the shaft. The secondary flow vectors in these plots show the flow sweeping in towards the center and up, as the flow follows the hull surface aft.

The nominal wake (flow without the propeller present) at the axial position of the propeller at $x/L = 0.9453$, is shown in Figs. 14 and 15. The white circle in the middle of the plots is the location of the propeller shaft, since no dummy hub was placed on the shaft. The inboard strut wake is significantly stronger here than at the earlier station, most likely due to both an interaction with the shaft wake, and the lack of flow acceleration from the propeller. The flow is also generally lower in velocity than at the upstream station, again most likely due to the lack of flow acceleration from the propeller.

The nominal wake just aft of the propeller at $x/L = 0.9603$, is shown in Figs. 16 and 17. At this plane, no obstructions to beam propagation exist, and the entire flow field is measured. The inner-

strut/shaft wake appears slightly stronger and the hull boundary layer is somewhat thicker than at the plane of the propeller. The turbulence level behind the hub is very high due to the lack of a faired dummy hub.

The flow at the same axial station, $x/L = 0.9603$, with the propeller is shown in Figs. 18 and 19. The propeller accelerates the axial flow to more than $1.2U_\infty$ with considerable swirl added to the flow. High turbulence exists not only behind the propeller hub, as with the nominal flow, but also at the edges of the propeller disk. There is considerable asymmetry in the flow out of the propeller in both swirl and axial velocity, with the highest velocities on the lower outboard side of the propeller and the lowest velocities on the upper inboard side of the propeller.

The effect of the propeller on the flow can better be seen in Fig. 20 which shows the difference in velocity between the propelled and unpropelled measurements. Here the color contours represent the change in axial velocity, while the vectors represent the change in the vertical and horizontal velocity components. The white areas in the picture show where there is no change in axial velocity between the propelled and unpropelled states; purple and red regions show where the axial velocity is lower in the propelled state; and yellow, orange, and blue regions show where the axial velocity is higher in the propelled state. The flow outside of the propeller jet is affected only slightly by the propeller, with the propeller causing slightly higher velocity on the outboard side and slightly lower velocity on the inboard side. Just above the propeller jet the flow is slowed more substantially. As one would expect, inside the propeller jet the flow is accelerated and swirl added. The highest change in axial velocity, however, is in the upper inboard side of the jet, where the propelled axial velocity is at a minimum. The decrease in axial velocity at the center of the jet with the propeller is due to the presence of the hub and fairwater on the propeller, which was not present in the unpropelled case.

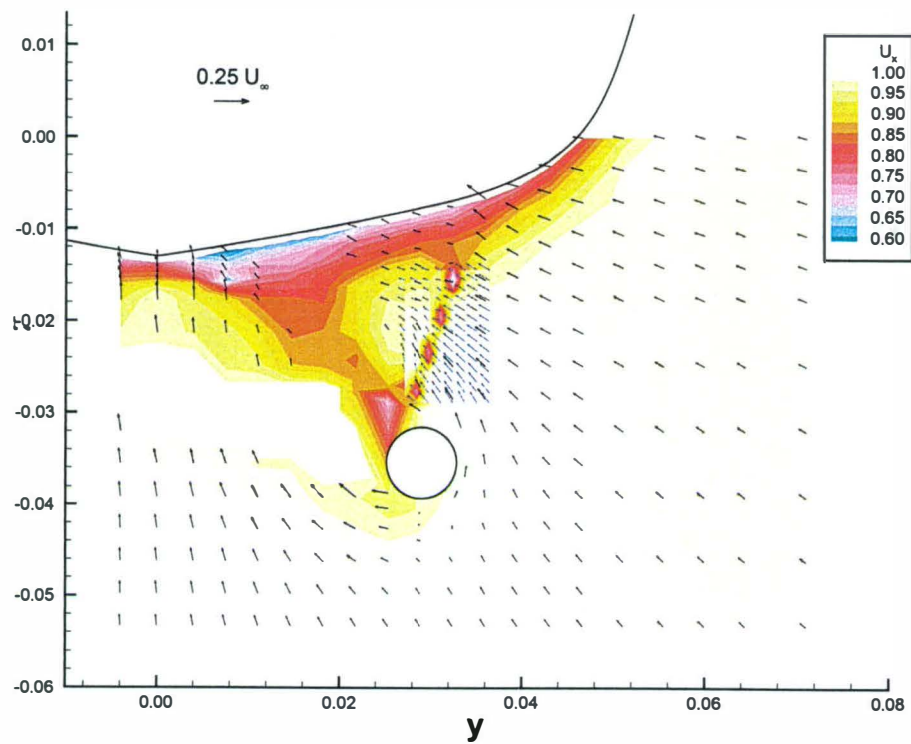


Figure 12 - Contours of axial velocity, $x/L = 0.9367$, propelled

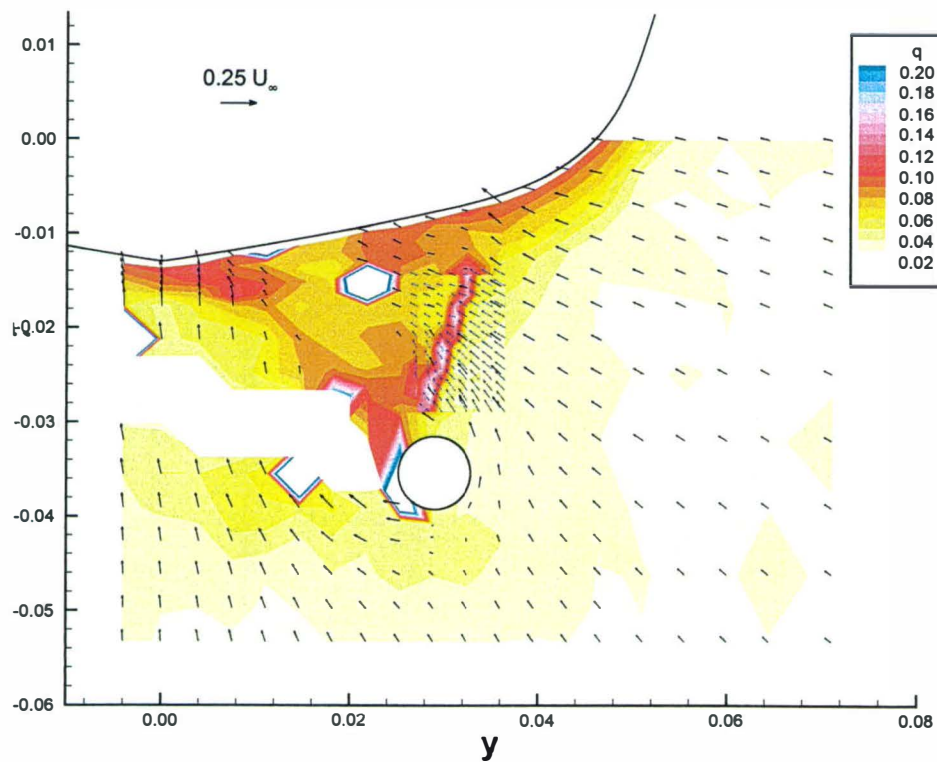


Figure 13 - Contours of rms velocity, $x/L = 0.9367$, propelled

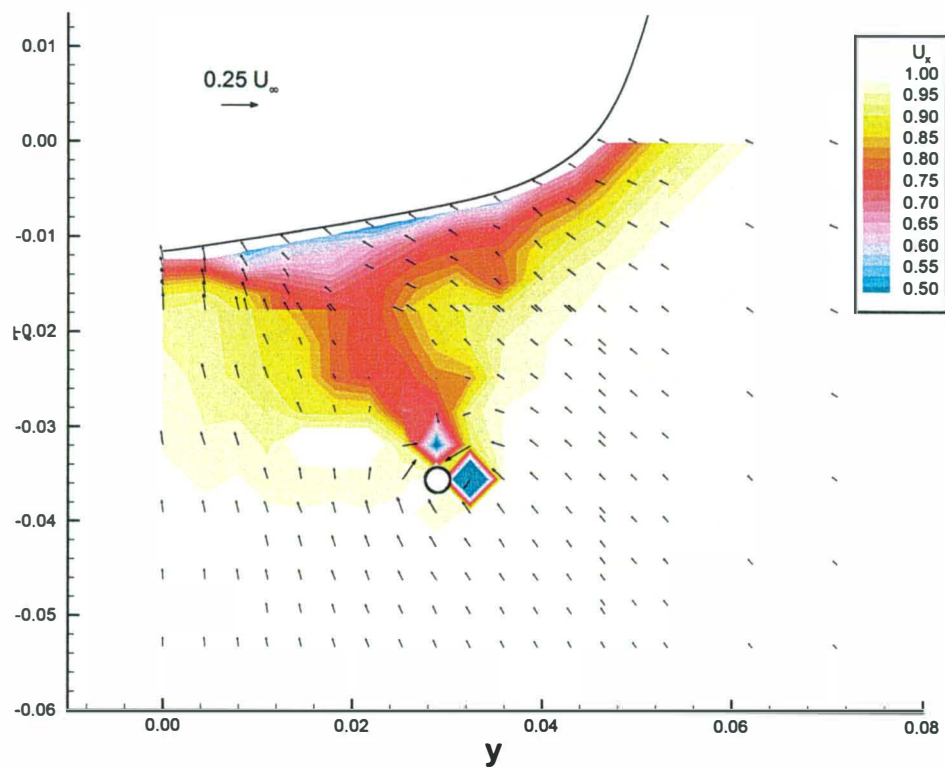


Figure 14 - Contours of axial velocity, $x/L = 0.9453$, nominal wake

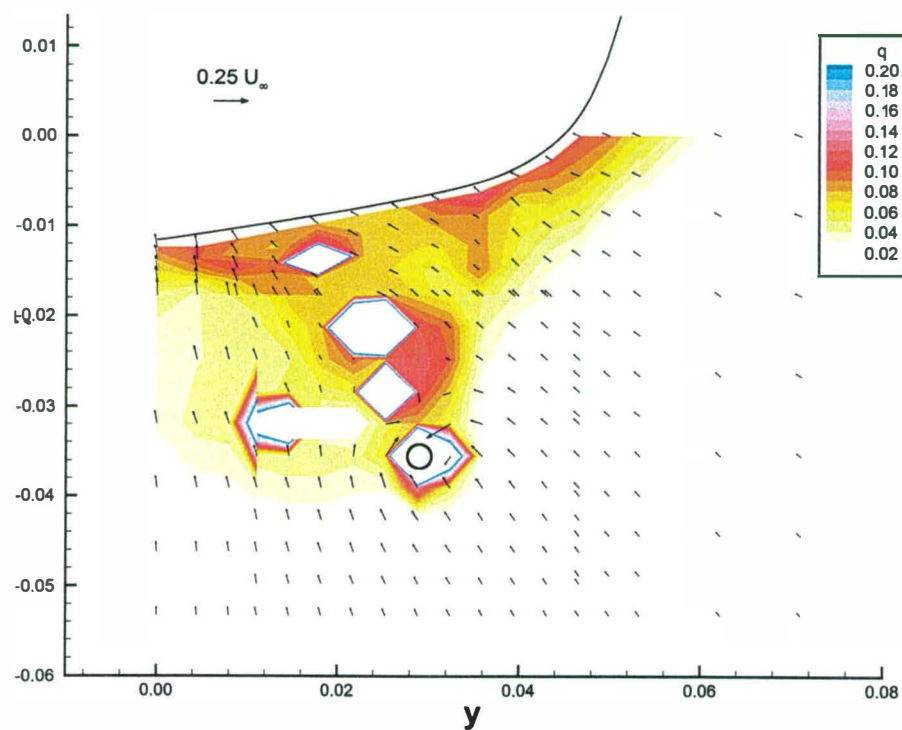


Figure 15 - Contours of rms velocity, $x/L = 0.9453$, nominal wake

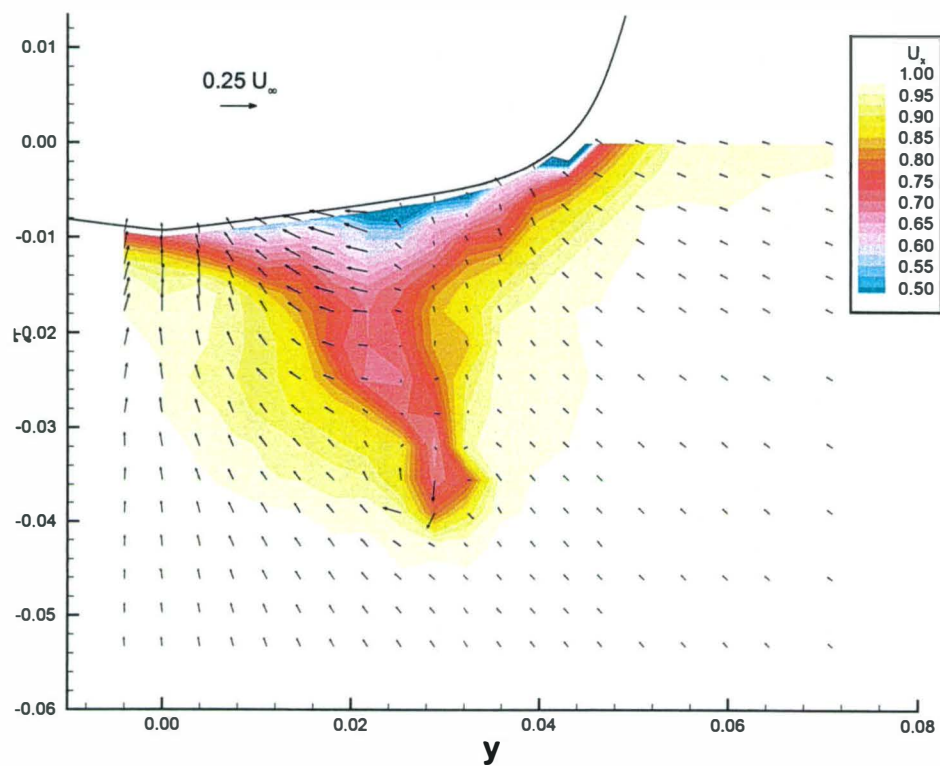


Figure 16 - Contours of axial velocity, $x/L = 0.9603$, nominal wake

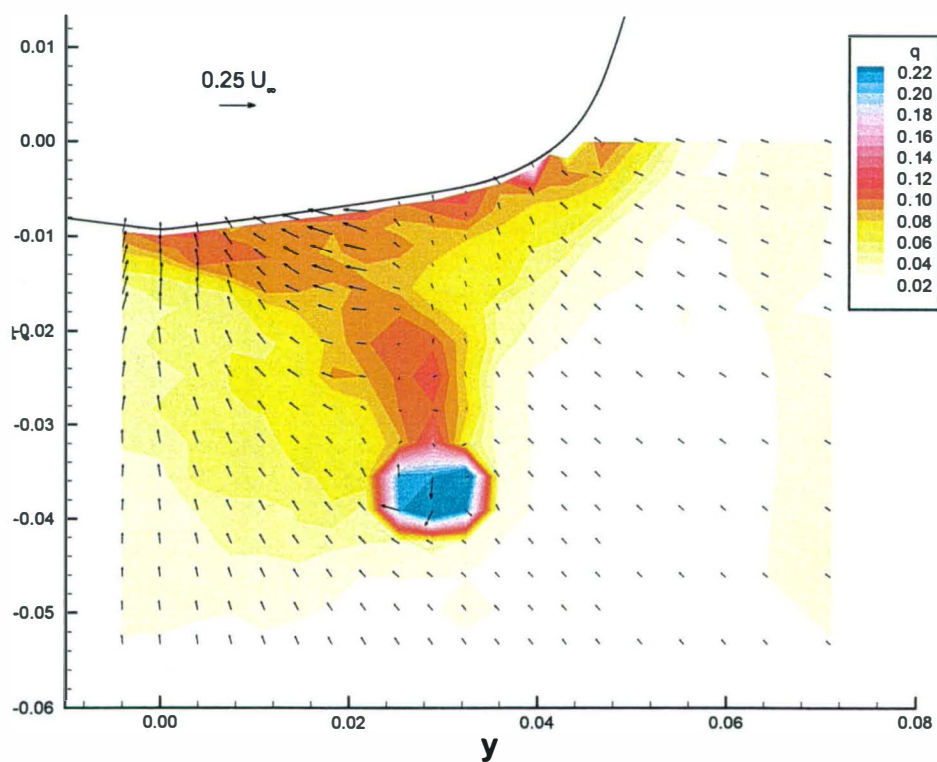


Figure 17 - Contours of rms velocity, $x/L = 0.9603$, nominal wake

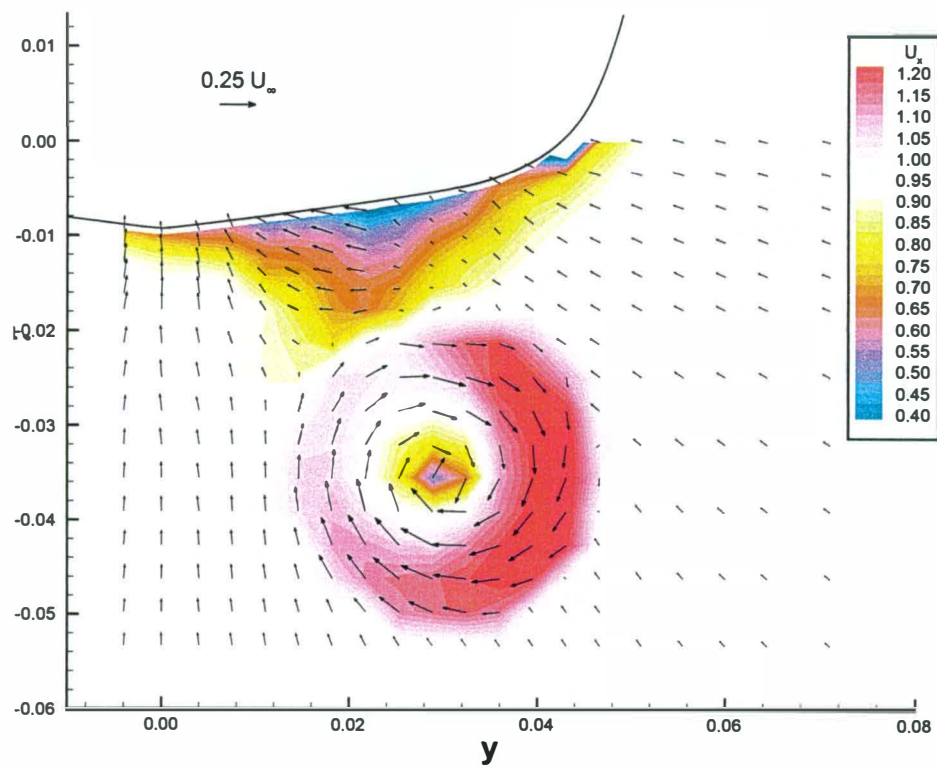


Figure 18 - Contours of axial velocity, $x/L = 0.9603$, propelled

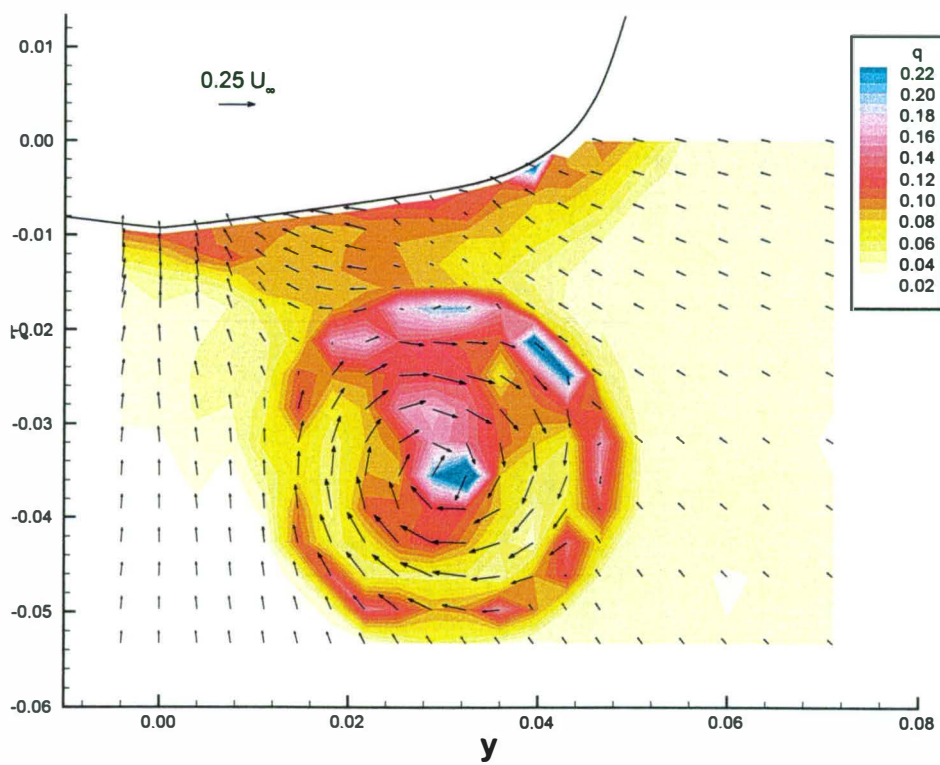


Figure 19 - Contours of rms velocity, $x/L = 0.9603$, propelled

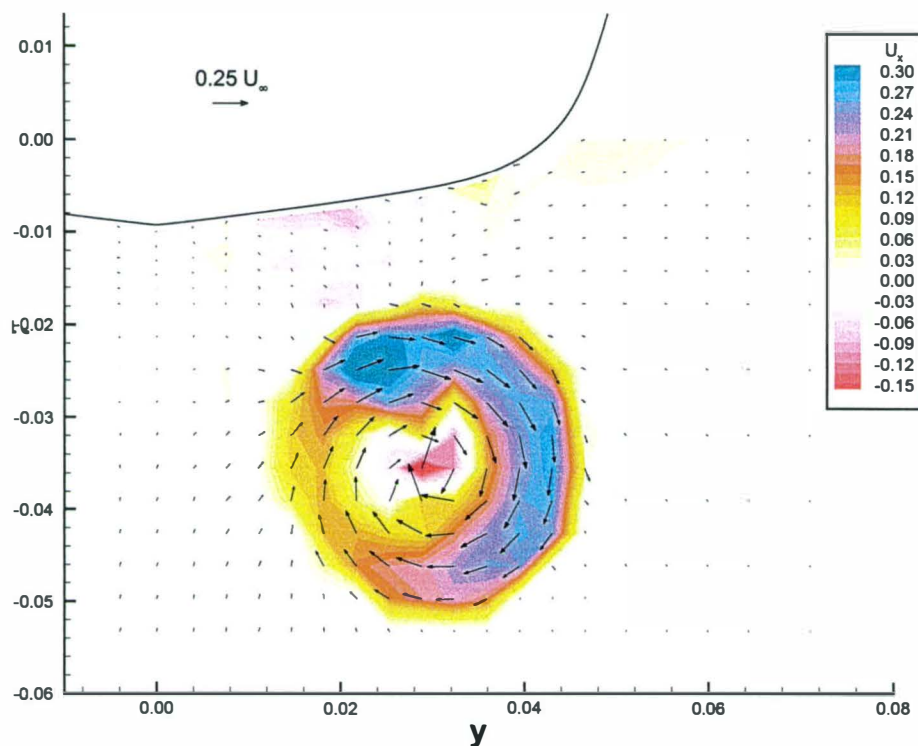


Figure 20 - Propelled minus nominal wake, $x/L = 0.9603$

CONCLUSIONS

The non-intrusive feature of laser doppler velocimetry means that velocities can be measured with and without the model propellers operating. This subsurface velocity data represents one of the most detailed sets of propeller plane data taken on a naval combatant hull form. These measurements will provide comprehensive validation data for the numerical hydrodynamics community to support code development.

A detailed uncertainty analysis was performed on this data. At almost all the measurement points, the dominant source of uncertainty is the precision uncertainty due to the long period fluctuations in the flow. Over most of the flow field, the turbulence is low, and the uncertainty in any velocity component is less than 0.8% of U_∞ . In high turbulence regions of the flow, such as the hull or propulsor wakes, the uncertainty can increase to 2.5% of U_∞ .

The velocities measured at upstream of the propeller plane shows the thickness of the boundary layer on the model. The LDV measurement grid was not fine enough to completely resolve the narrow wakes from the shaft struts. Even when a finer grid was used to measure the region of the outboard strut, the contours are still imprecise. At the nominal wake plane there is no flow acceleration from the propeller. This results in a strengthening of the inboard strut wake as it interacts with the shaft wake. When the nominal wake is measured aft of the propeller plane, the strut/shaft wake is stronger and the hull boundary layer has thickened. Measurements aft of the propeller plane with the propeller operating reveals an acceleration of axial flow to more than $1.2U_\infty$ with considerable swirl added to the flow.

BLANK

INITIAL DISTRIBUTION

Copies

1 ONR
 1 333 (Pat Purtell)

1 University of Michigan
 1 Robert Beck

2 University of Iowa
 1 Frederick Stern
 1 Joseph Longo

1 SAIC/San Diego
 1 Don Wyatt

1 Naval Surface Warfare Center,
 Panama City
 1 Mark Hyman

1 ARL
 Eric Patterson

1 DTIC

Center Distribution

Copies	Code	Name
1	3442	Library
1	5030	Jessup
	5010 w/o encl	
13	5060	Walden
1	5200	Karafiath
3	5200	Cusanelli
2	5200	Office Files
15	5400	Chesnakas
1	5400	Black
1	5400	Gorski
1	5600	Fu